Journal of Reproduction and Development, Vol. 63, No 2, 2017

—Original Article—

Visualization of the spatial arrangement of nuclear organization using three-dimensional fluorescence *in situ* hybridization in early mouse embryos: A new "EASI-FISH chamber glass" for mammalian embryos

Masataka NAKAYA[1)*], Hideyuki TANABE[2)*], Shingo TAKAMATSU[3)], Misaki HOSOKAWA[3)] and Tasuku MITANI[1, 4)]

[1)]*Graduate School of Biology-Oriented Science and Technology, Kindai University, Wakayama 649-6493, Japan*
[2)]*Department of Evolutionary Studies of Biosystems, School of Advanced Sciences, SOKENDAI (The Graduate University for Advanced Studies), Kanagawa 240-0193, Japan*
[3)]*Department of Biology-Oriented Science and Technology, Kindai University, Wakayama 649-6493, Japan*
[4)]*Institute of Advanced Technology, Kindai University, Wakayama 642-0017, Japan*

Abstract. The fertilized oocyte begins cleavage, leading to zygotic gene activation (ZGA), which re-activates the resting genome to acquire totipotency. In this process, genomic function is regulated by the dynamic structural conversion in the nucleus. Indeed, a considerable number of genes that are essential for embryonic development are located near the pericentromeric regions, wherein the heterochromatin is formed. These genes are repressed transcriptionally in somatic cells. Three-dimensional fluorescence *in situ* hybridization (3D-FISH) enables the visualization of the intranuclear spatial arrangement, such as gene loci, chromosomal domains, and chromosome territories (CTs). However, the 3D-FISH approach in mammalian embryos has been limited to certain repeated sequences because of its unfavorable properties. In this study, we developed an easy-to-use chamber device (EASI-FISH chamber) for 3D-FISH in early embryos, and visualized, for the first time, the spatial arrangements of pericentromeric regions, the ZGA-activated gene (*Zscan4*) loci, and CTs (chromosome 7), simultaneously during the early cleavage stage of mouse embryos by 3D-FISH. As a result, it was revealed that morphological changes of the pericentromeric regions and CTs, and relocation of the *Zscan4* loci in CTs, occurred in the 1- to 4-cell stage embryos, which was different from those in somatic cells. This convenient and reproducible 3D-FISH technique for mammalian embryos represents a valuable tool that will provide insights into the nuclear dynamics of development.

Key words: Chromosome territory, Gene locus, Pericentromeric region, Three-dimensional fluorescence *in situ* hybridization (3D-FISH)

(**J. Reprod. Dev. 63:** 167–174, 2017)

Fertilization is a unique event that generates a zygote with new hereditary information, which consists of a biparental genome resulting from the fusion of an oocyte with sperm. A fertilized oocyte is transcriptionally silent and initiates embryonic development using maternal factors. At the appropriate developmental stage, the embryo reactivates its resting genome via chromatin remodeling to acquire totipotency, termed zygotic gene activation (ZGA). The nuclear architecture during this process is quite different from that of somatic cells, and in recent years, the nuclear dynamics governing genomic function in embryonic development have attracted increasing research attention [1, 2]. In somatic cells, centromeric and pericentromeric regions in each chromosome comprise highly condensed heterochromatin, named chromocenters, and are interspersed along the nucleus. By contrast, during the 1- to mid-2-cell stages of mouse embryos, pericentromeric regions are converted to a state wherein the chromatin is loosened and are distributed around the "nucleolus-like bodies (NLBs)". Thereafter, at the late-2-cell stage, pericentromeric regions condense to form somatic cell-type chromocenters [3]. Upon ZGA, the expression of repeated sequences in pericentromeric regions is triggered [4]. In addition to the alteration of regional status within a chromosome, individual chromosomes are unwound and become highly compartmentalized in the regions of the nucleus, and such a region is termed a "chromosome territory (CT)" [5]. The intranuclear configuration of CTs is associated with their size and genetic density [6, 7], or cell differentiation [8]. Studies on CTs and gene loci are underway in somatic cells such as T lymphocytes; however, little is known about the dynamics and roles of CTs in development and differentiation. Previously, it was demonstrated that during the development of the mouse limb bud, the promoter region of the *Sonic Hedgehog* (*Shh*) gene interacts physically with its enhancer, mammalian fish conserved sequence 1 (MFCS1), a cis-regulatory element that acts over a long-range at the specific embryonic stage in both the anterior and posterior limb bud cells. However, the *Shh* loci relocate to the surface region of CT5 only in the posterior limb bud cells where *Shh* expression is active [9]. Higher-order arrange-

Received: December 12, 2016
Accepted: January 4, 2017
Published online in J-STAGE: February 11, 2017

Correspondence: T Mitani (e-mail: mitani@waka.kindai.ac.jp)
* Nakaya M and Tanabe H contributed equally to this work.

ments of CTs also change dynamically after ZGA [10]. Therefore, a study of the dynamics of higher-order nuclear structures during the process of maternal to zygotic transition (MZT) would help to reveal the chromosomal environment for genomic function in embryonic development.

Three-dimensional fluorescence *in situ* hybridization (3D-FISH) is a powerful tool to visualize spatial arrangements in a nucleus, such as gene loci, chromosomal domains, and CTs in interphase cells. However, 3D-FISH in oocytes and early embryos in mammals has been confined to reports concerning the repeated sequences in centromeres and telomeres, as well as rDNA [3, 4, 11, 12], because of the unique properties attributable to a large spherical cell with a diameter of 100 µm, which interferes with the permeation/elution of probes because of the large amount of ooplasm/cytoplasm and requires fine manipulation skill using micro-capillaries under microscopes throughout the process of FISH. In this study, we devised a new "EASI-FISH chamber glass" for 3D-FISH in early embryos, which enabled convenient and reproducible anchoring of the embryo onto the coverslip, while retaining its steric structure throughout the FISH process. Using this method, we demonstrated examples of chromatin dynamics during the early cleavage stages of mouse embryos. As a 3D-FISH model, we focused on the Zinc finger SCAN domain containing 4 (*Zscan4*) gene. A considerable number of ZGA-activated genes are located in the chromatin domains near centromeres [13]. Mouse *Zscan4*, which is located next to the pericentromeric G-positive banded region of chromosome 7, is expressed exclusively at the late-2-cell stage, and diminishes promptly thereafter. *Zscan4*-knockdown zygotes show delayed progression beyond the 2-cell stage and post-implantation development fails to proceed [14]. This indicated that *Zscan4* expression is closely related to ZGA. *Zscan4* is also expressed partly in embryonic stem (ES) cells [14]. Besides *Zscan4*, ribosomal protein S19 (*Rps19*) maps to the anterior region of chromosome 7, and *Rps19*-deficient embryos showed developmental arrest until the blastocyst stage [15]. In addition, it has been revealed that genes located near the pericentromeric regions, such as Cofilin 1 (*Cfl1*) on chromosome 19, play an important role in compaction [16]. Using our 3D-FISH technique, we visualized successfully the dynamics of ZGA-activated gene loci that correlated with pericentromeric regions and CTs for the first time in early cleavage stage mouse embryos.

Materials and Methods

Animals

All mice (B6D2F1 strain) were purchased from Japan SLC (Shizuoka, Japan) at 8 weeks of age and maintained in light-controlled and air-conditioned rooms. This study was carried out in strict accordance with the recommendations in the Guidelines of Kindai University for the Care and Use of Laboratory Animals. The protocol was approved by the Committee on the Ethics of Animal Experiments of Kindai University (Permit Number: KAAT-23-002).

Embryo collection and culture

The procedures for *in vitro* fertilization were performed according to a previously described method [17, 18]. In brief, spermatozoa were collected from the cauda epididymis of male mice. The sperm suspension was incubated in Human Tubal Fluid medium (HTF) (ARK-Resource, Kumamoto, Japan) for 1.5 h at 37°C under 5% CO_2 in air to allow for capacitation. Oocytes were collected from the excised oviducts of female mice that had been superovulated by intraperitoneal injection of pregnant mare's serum gonadotropin (PMSG, 7.5 IU; Serotropin, ASKA Pharmaceutical, Tokyo, Japan) followed 48 h later by intraperitoneal injection of human chorionic gonadotropin (hCG, 7.5 IU; ASKA Pharmaceutical). The sperm suspension was added into the HTF medium containing the oocytes. Thereafter, morphologically normal fertilized oocytes were recovered and cultured in KSOM (potassium-supplemented simplex optimized medium; ARK-Resource) at 37°C under 5% CO_2 in air. Embryos at the 1-, 2-, and 4-cell stages were collected at 24, 36, and 48 h post-insemination (hpi), respectively. Embryos were treated with acidified Tyrode's solution (Irvine Scientific, Santa Ana, CA, USA) to remove the zona pellucida, and rinsed in phosphate buffered saline (PBS) containing 0.3% polyvinyl pyrrolidone (PVP; Wako Pure Chemical Industries, Osaka, Japan). Thereafter, they were fixed in 4% paraformaldehyde (PFA; Wako Pure Chemical Industries) for 15 min, rinsed in PBS, and stored in 0.3% PVP/PBS before FISH.

Cell culture

Somatic cells (fibroblasts) were collected from the tail tip tissue of B6D2F1 mice. The tissues were minced and treated with 0.25% trypsin–0.53 mM EDTA solution (Invitrogen, Carlsbad, CA, USA) at 37°C for 10 min to dissociate into single cells. Fibroblasts were cultured in Dulbecco's modified Eagle's medium (DMEM; Invitrogen) supplemented with non-essential amino acids (NEAA; Invitrogen) and 10% fetal bovine serum (FBS; Biowest, Nuaillé, France) at 37°C under 5% CO_2 in air. Mouse ES cells of the R-CMTI-2A line (C57/BL6-derived mouse ES cell line; DS Pharma, Osaka, Japan) were cultured in DMEM/NEAA + 15% FBS with leukemia inhibitory factor (LIF) (ESGRO, 1,000 units/ml; Millipore, Darmstadt, Germany) at 37°C under 5% CO_2 in air. For 3D-FISH analysis, fibroblasts and ES cells were plated on gelatinized coverslips (24 mm × 60 mm, MATSUNAMI, Osaka, Japan) under the same culture conditions. Thereafter, cells at sub-confluence were fixed with 4% PFA at room temperature (RT: 18–22 °C) for 15 min, and then were rinsed and stored in PBS before FISH.

Chamber device for 3D-FISH of early embryos

Coverslips (24 mm × 60 mm, MATSUNAMI) for the 3D-FISH chamber were soaked in absolute methanol. To retain the 3D structure of nuclei from any deforming pressures, a frame of approximately 100 µm in depth was formed by affixing double-layered clear patches (TA-3N, KOKUYO, Osaka, Japan) on the center of delipidated coverslips. To adhere the embryos firmly to the coverslips, the inside of the frame was coated with 20 µl of poly-L-lysine hydrobromide (PLL; P1399, Sigma-Aldrich, St. Louis, MO, USA) at a concentration of 5 mg/ml in 125 mM boric acid solution (pH 7) for 2 h at RT. PLL-coated coverslips were rinsed in distilled water and dried overnight in air at RT (Fig. 1).

Probe preparation

To delineate mouse chromosome 7, we used whole chromosome painting probes kindly provided by Dr. Michael Speicher (Institute

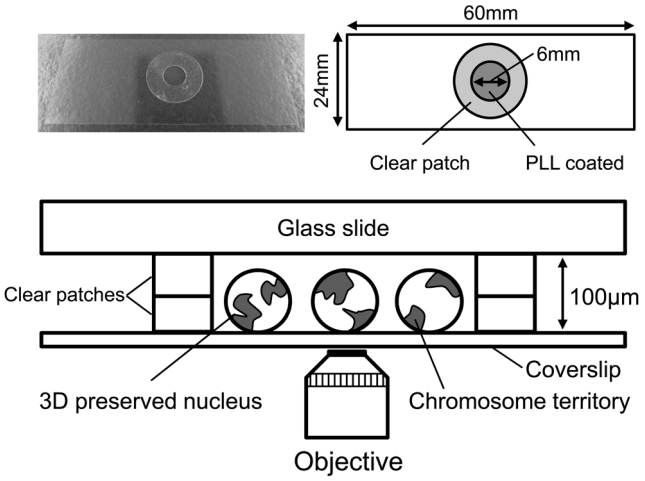

Fig. 1. Three-dimensional fluorescence *in situ* hybridization (3D-FISH) chamber for preimplantation embryos. Upper left; an actual object of the chamber. Upper right; plane view of the chamber. A coverslip (24 mm × 60 mm) is affixed to double-layered clear patches of 6 mm inside diameter. Lower; side view. The nuclei of the embryos in the space between the coverslip and the glass slide have a preserved steric structure throughout the whole process of 3D-FISH. The chamber makes it possible to maintain the nuclear morphology of the embryos and allows access of certain probes into the chromatin.

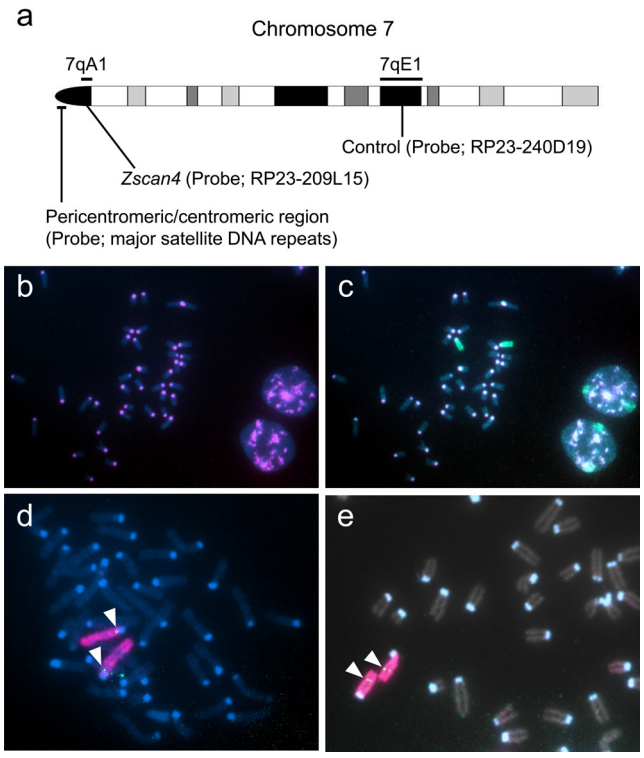

Fig. 2. Confirmation of the fluorescence *in situ* hybridization (FISH) system detection with the probes used in this study. Two-dimensional-FISH analysis was performed in metaphase spreads prepared from mouse fibroblasts. (a) Idiogramatic illustration of mouse chromosome 7 with the cytogenetic localization of probes. The bacterial artificial chromosome (BAC) clones RP23-209L15 and RP23-240D19 were selected for the *Zscan4* gene region located on chromosome band 7qA1 and another DNA segment on chromosome band 7qE1, respectively. (b, c) Images of the mouse chromosome 7 painting probe combined with the major satellite DNA repeats. Nuclear DNA was counterstained with DAPI (2-(4-amidinophenyl)-1H-indole-6-carboxamidine) and appears blue. (b) The major satellite DNA probe that consists of part of the 234-bp repeats was detected on the pericentromeric/centromeric regions, as indicated in red. (c) The same metaphase image as in (b) with three-color staining. Whole chromosome 7 painting probe (green) was detected on the two specific metaphase chromosome 7 regions. The major satellite DNA probe (red) was actually shown in white (overlaid with red, green, and blue). (d) Three-color image with the locus-specific probe for *Zscan4* (green) and whole chromosome 7 painting probe (red). Both of the green signals (arrowheads) for *Zscan4* were detected on the specific sites next to the pericentromeric regions identified with condensed heterochromatin by DAPI counterstaining. (e) Four-color image with the site-specific probe for RP23-240D19 (green), whole chromosome 7 painting probe (red), and the major satellite DNA probe (blue). Nuclear DNA was counterstained with DAPI (gray). Both of the green signals (arrowheads) for RP23-240D19 were detected on the addressed sites.

of Human Genetics, Medical University of Graz, Graz, Germany). An idiogramatic illustration of mouse chromosome 7 with the cytogenetic localization of probes is presented in Fig. 2a. The probe for chromosome segments extending over pericentromeric and centromeric regions was prepared by PCR from mouse major satellite DNAs with the primers 5′-CCC AAG CTT GAA ATG TCC ACT-3′ and 5′-CCC AAG CTT TTT CTT GCC ATA-3′ [19]. The probe for *Zscan4* was prepared from a specific bacterial artificial chromosome (BAC) clone (MMU7; BAC clone RP23-209L15; purchased from Advanced Geno Techs, Ibaraki, Japan). We used another BAC-DNA for RP23-240D19 localized on the G-positive banded region on 7qE1 as a control probe for *Zscan4*. There are no active genes during the embryonic stages within RP23-240D19. The DNA probes for chromosome 7 and pericentromeric/centromeric regions (major satellite) were labeled by degenerated oligonucleotide primed (DOP)-PCR [20] in the presence of digoxigenin-11-dUTP (DIG-11-dUTP) (Roche, Basel, Switzerland). The DNA probes for *Zscan4* and RP23-240D19 were labeled by DOP-PCR in the presence of dinitrophenyl-11-dUTP (DNP-11-dUTP) (NEL 551, PerkinElmer, Waltham, MA, USA). The labeled DNA probes were suspended at a final concentration of 50 ng/μl together with a 20-fold excess of unlabeled mouse *Cot-1* DNA (Invitrogen) in 50% formamide/10% dextransulfate/2 × SSC (Invitrogen). To validate the specificity of the probes, DNA-FISH on metaphase chromosome spreads of mouse fibroblast cells was performed and definite signals for pericentromeric/centromeric regions (Fig. 2b, c), *Zscan4* (Fig. 2d), RP23-240D19 (Fig. 2e), and chromosome 7 (Fig. 2c–e) were obtained by specific visualization of the addressed regions and gene loci at the expected chromosomal positions, where the location of *Zscan4* and RP23-240D19 are indicated as MMU-7qA1 and MMU-7qE1, respectively.

3D-FISH

3D-FISH and probe detection were performed according to a previously described method, with modifications to optimize the

procedure for early embryos (Supplementary Fig. 1: online only) [7, 9, 21–23]. Unless otherwise noted, specimens were treated at RT. The fixed embryos were placed into a chamber frame with 20 µl of PBS using a micro-capillary, and then incubated for 1 h at RT for adhesion. The coverslips mounted with cultured cells were treated in similarly thereafter. For permeabilization, the chamber was treated with 0.5% saponin (Sigma-Aldrich) and 0.5% Triton X-100 (Sigma-Aldrich) in PBS for 30 min and then incubated in 20% glycerol (Nacalai Tesque, Kyoto, Japan) in PBS for at least 30 min. The chamber was then frozen in liquid nitrogen (LN_2) for 30 sec followed by freezing-thawing in 20% glycerol five times. The chamber was rinsed with PBS for 5 min twice, treated with 0.1 N HCl (Wako Pure Chemical Industries) for 10 min, rinsed in PBS for 3 to 5 min, and then treated with 0.002% pepsin (Roche) in 0.01 N HCl at 37°C for appropriate periods depending on the embryonic stages (1-cell: 15–30 sec, 2- to 4-cell: 60 sec, cultured cells: 30 sec). The chamber was washed with 0.05 M $MgCl_2$ (Nacalai Tesque) in PBS for 5 min twice followed by an additional wash in PBS. The chamber was treated with 0.5% saponin and 0.5% Triton X-100 in PBS for 60 min, washed in PBS for 5 min twice, and fixed again with 1% PFA/PBS (pH 7.0) for 10 min. The chamber was washed in PBS for 5 min and in 2 × SSC for 5 min, and stored in 50% formamide (Wako Pure Chemical Industries)/2 × SSC at 4°C until hybridization. For hybridization, the chamber was applied with 6 to 7 µl of predenatured probes, covered with a round coverslip (Thermo Fisher Scientific, Waltham, MA, USA), and then mounted with Fixogum Rubber Cement (11FIXO0125, MP Biomedicals, Santa Ana, CA, USA). The specimen containing the embryos or cells was denatured at 80.5°C for 4 min and hybridized at 37°C for at least 5 days. The specimen was washed in 2 × SSC followed by 0.1 × SSC at 62.5°C three times for 5 min each. After washing in 4 × SSC with 0.2% Tween-20 (SSCT), the specimen was blocked with 5% BSA in 4 × SSCT at 37°C for 30 min. Both mouse anti-digoxigenin (DIG) IgG (D8156, Sigma-Aldrich) and rabbit anti-dinitrophenyl (DNP) IgG (D9656, Sigma-Aldrich) with RNase A (R4875, Sigma-Aldrich) were diluted together to 1:200 (RNase A; 100 µg/ml) in 5% BSA in 4 × SSCT and incubated with the specimen at 37°C for 1 h. After washing in 4 × SSCT at 37°C twice, the specimen was incubated with goat anti-mouse IgG conjugated with Cy5 (1:100) (A10524, Molecular Probes, USA), sheep anti-mouse IgG antibody conjugated with Cy3 (1:100) (515-165-062, Dianova/Jackson Immuno Research Lab, West Grove, PA, USA), and/or goat anti-rabbit IgG conjugated with Alexa Fluor 488 (1:100) (11008, Molecular Probes) with RNase A (100 µg/ml) in 5% BSA in 4 × SSCT at 37°C for 1 h. After washing in 4 × SSCT at 37°C twice, the specimen was counterstained with propidium iodide (PI) or TO-PRO-3 (T3605, Thermo Fisher Scientific).

3D image analysis

Specimens were scanned with an axial distance of 200 nm using a three-channel laser scanning confocal microscope (Carl Zeiss LSM 510 META or LSM 880) equipped with a 63 ×/1.4 Plan-Apochromat objective. For each optical section, images were acquired sequentially for all three fluorochromes (Cy3, Cy5, and Alexa Fluor 488). The nuclear periphery was reconstructed from threshold images of the DNA counterstain (PI, DAPI (2-(4-amidinophenyl)-1H-indole-6-carboxamidine), or TO-PRO-3). Stacks of 12–16 bit gray-scale two-dimensional images were obtained with a pixel size of 66 nm. Displayed overlays of confocal images were processed with Adobe Photoshop 5.5 or Carl Zeiss ZEN lite 2012. Three-dimensional reconstructions of hybridized nuclear image stacks were created using Amira 3.1.1 TGS (http://www.amiravis.com/) software. To investigate whether *Zscan4* loci were located on the surface of CT7 during the early embryonic stages, we calculated the frequencies of FISH signals of *Zscan4* loci located on the surface of CT7 using the profiling function of LSM 5 Image Browser or ZEN lite software. Each detected FISH signal of *Zscan4* on CT7 at the particular optical section of the image stacks was applied for profiling to visualize the graphical data and classified as to whether peaks of FISH signals were placed inside or on the surface of CT7. In addition, the average volume of CT7 was measured using Imaris 7.4.2 software for the 1-, 2-, and 4-cell stages, as well as ES cells and fibroblasts for reference.

Statistical analysis

We measured the positioning of *Zscan4* gene locus in CT7 and the volume of CT7 in the early embryos, ES cells, and fibroblasts. The Tukey-Kramer test was used to determine the significance of the differences in *Zscan4* positioning and the volume of CT7s. The statistical analysis software StatView version 5.0 (SAS Institute, Cary, NC, USA) was used.

Results

Devising an easy-to-use chamber glass for 3D-FISH in early embryos

To develop a 3D-FISH procedure adapted for early embryos, we made a new chamber device with a frame-like bank on a poly-L-lysine coated coverslip, which enabled embryos to adhere and retain their 3D-structure (Fig. 1). The chamber device also made it easy to put the embryos together in a small area and facilitated FISH protocol with easy handling (Supplementary Fig. 1). As to the stability of specimens, the embryos adhered firmly and did not come off easily by handling throughout the 3D-FISH process and during freezing in LN_2. The frame-like bank was resistant to a high temperature of 100°C for 15 min. Using this chamber device, we undertook 3D-FISH in early embryos to examine whether the nucleus retained its spatial structure and presented definite FISH signals. As a result, the embryos firmly adhered to the chamber surface, which made it possible to treat them with a sufficient volume of buffer solutions, which increased the permeability of the specimens and aided the hybridization of probes. This 3D-FISH approach demonstrated that the spatial structure of the nucleus, defined by DNA staining with TO-PRO-3 or PI, was retained and that the pericentromeric/centromeric regions, certain gene loci, and CTs in the nucleus, were visualized specifically by multicolor DNA-FISH with little loss of specimens (Fig. 3). Accordingly, we named this chamber device the "EASI (Embryo Anchoring for Spatial Information)-FISH" chamber. Using LSM 510 META or LSM 880 microscopes, specific fluorescent signals for pericentromeric/centromeric regions, *Zscan4* loci, and CT7s were detected in the embryos at the 1-, 2-, and 4-cell stages, respectively, as well as in ES cells and fibroblasts (Fig. 3). From these integrated image stacks, 3D images of the nuclear structure were reconstructed (Fig. 4).

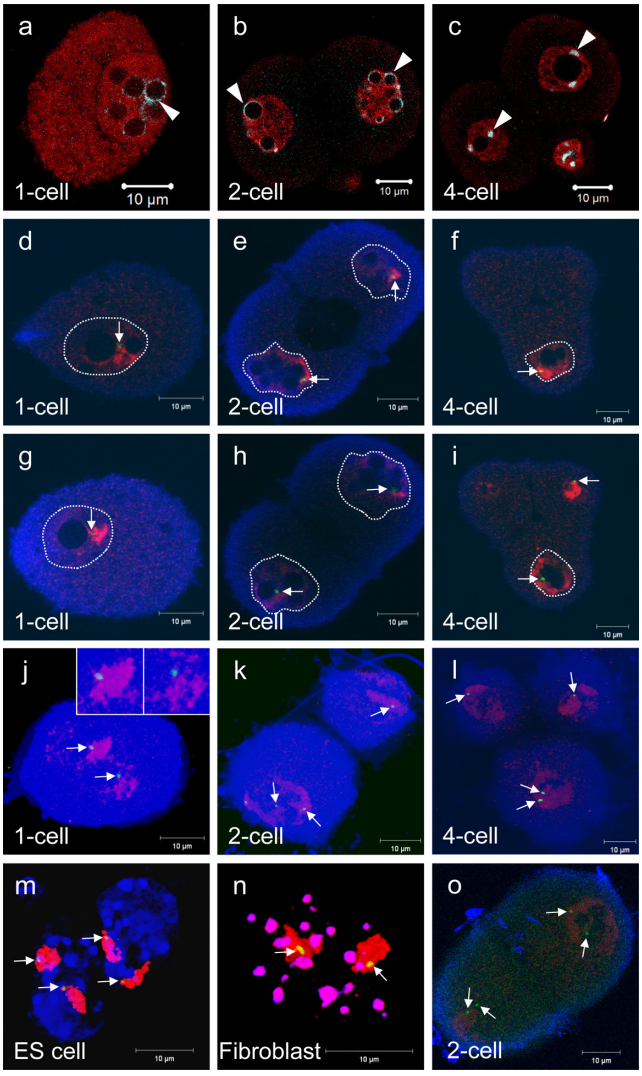

Fig. 3. Spatial distribution of pericentromeric/centromeric regions, *Zscan4* loci, and chromosome territory (CT) 7 after three-dimensional fluorescence *in situ* hybridization (3D-FISH). (a–c) Each image shows a single optical section of image stacks from the 1- to 4-cell stages, respectively. Pericentromeric/centromeric regions (arrowheads) are represented in light blue and nuclei are counterstained with PI in red. Pericentromeric/centromeric regions partially surround nucleolus-like bodies (NLBs) both at the 1-cell and 2-cell stages, but become condensed to form chromocenters beside NLBs at the 4-cell stage. (d–f) Images from a single optical section of image stacks for CT7s (red), *Zscan4* loci (green) (arrows), and TO-PRO-3 (blue) are shown for the 1- to 4-cell stages, respectively. CT7 shows an enlarged and deformed shape at the periphery of NLBs during the early cleavage stage. The edge of each nucleus is delineated by a white dotted line. (g–i) The images from the same nuclei as in (d–f) but from different optical sections. Another CT7 and *Zscan4* locus are shown in each image. (j–l) The projection images from the same nuclei as in (d–g), (e–h), and (f–i), respectively. *Zscan4* loci are indicated by arrows. Insets in (j) are magnified images of the *Zscan4* locus and CT7. (m) A projection image of nuclei from embryonic stem (ES) cells. CT7s, *Zscan4* loci, and TO-PRO-3 are represented in red, green (arrows), and blue, respectively. (n) A projection image of as single nucleus from a fibroblast. CT7s, *Zscan4* loci, and pericentromeric/centromeric regions are represented in red, green (arrows), and purple, respectively. Note that pericentromeric/centromeric regions form dotted chromocenters and CT7s appear as relatively small lump shapes in the nuclei in ES cells (m) and fibroblast (n). (o) A projection image from the 2-cell nuclei. CT7, RP23-240D19, and TO-PRO-3 are represented in red, green (arrows), and blue, respectively. Scale bar; 10 μm.

Spatial distribution of pericentromeric/centromeric regions, gene loci of Zscan4, and CT7s

We investigated the spatial arrangement of a gene locus located next to the pericentromeric region of the harboring chromosome. The early embryos, ES cells, and fibroblasts from mice were fixed in 4% PFA for preservation of their 3D nuclear structure and were examined by 3D-FISH using the EASI-FISH chamber. The specimens were analyzed using a confocal laser scanning microscope and computational 3D-imaging. As a result, we visualized the pericentromeric/centromeric regions, *Zscan4* loci, and CT7s in the nuclei of early embryos successfully, similarly to the ES cells and fibroblasts (Fig. 3).

Pericentromeric/centromeric regions were detected by DNA-FISH with major satellite probes together with DNA counterstaining with PI in the nuclei of the early embryos (Fig. 3a–c). Although in fibroblasts, the pericentromeric/centromeric regions (purple) were condensed and integrated into the spotted chromocenters in the nuclei (Fig. 3n), the embryos showed unique kinetics of reorganization of the pericentromeric/centromeric regions (light blue) (Fig. 3a–c). In the 1- and 2-cell stage embryos, the pericentromeric/centromeric regions were distributed uniquely in a sphere surrounding the NLBs and then remodeled to a chromocenter-like structure at the 4-cell stage (Fig. 3a–c), as previously reported [3, 12]. Such a reorganized distribution is in distinct contrast to the characteristic pattern of pericentromeric heterochromatin dots in fibroblasts (Fig. 3n). CT7s in the nuclei were visualized successfully using a chromosome painting probe (red), together with DNA counterstain TO-PRO-3 (blue) (Fig. 3d–o). In ES cells and fibroblasts, CT7s appeared as relatively small lump shapes in the nuclei (Fig. 3m, n; Fig. 4d); however, those in the nuclei of the embryos were enlarged and had deformed shapes (Fig. 3d–l, o; Fig. 4a–c, e). Interestingly, in the 1- to 4-cell stage embryos, CT7s gathered around NLBs were unlike those of fibroblasts. Three-dimensional positions of *Zscan4* loci and RP23-240D19 were detected by multicolor DNA-FISH with BAC clone probes (green) combined with chromosome 7 painting probe (red), together with DNA counterstaining TO-PRO-3 (blue) in the

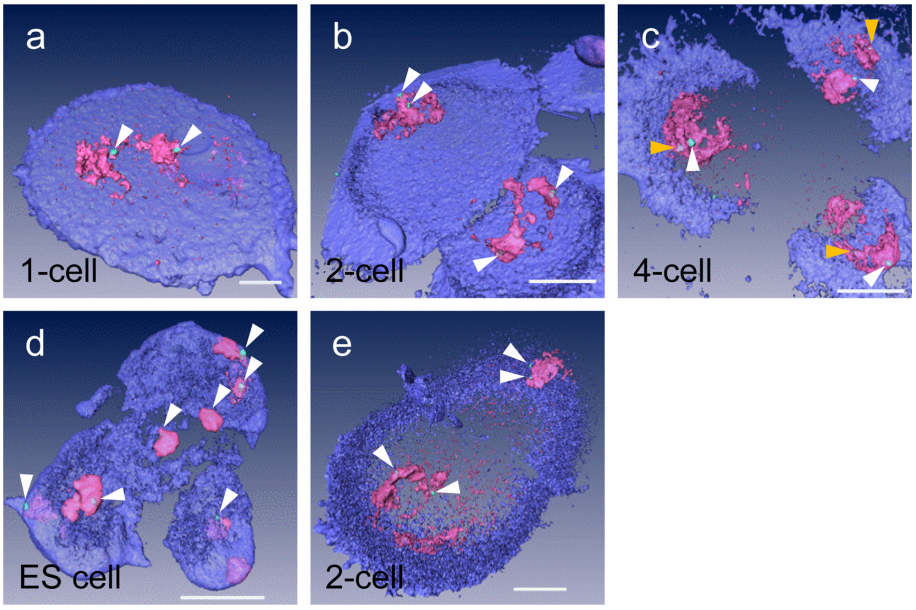

Fig. 4. Three-dimensional reconstruction images for the 1-cell (a), 2-cell (b, e) and 4-cell (c) stages, and embryonic stem (ES) cells (d), respectively, from confocal image stacks scanned after three-dimensional fluorescence *in situ* hybridization (3D-FISH) with chromosome territory (CT) 7 (red), *Zscan4* loci (green), and counterstained nuclear DNA (blue), made by Amira 3.1.1 TGS software. Several *Zscan4* loci are localized in the interior of CT7, as indicated by the yellow arrowheads in (c). (e) 3D reconstruction image for the 2-cell stage from confocal image stacks scanned after 3D-FISH with CT7 (red), RP23-240D19 (green), and counterstained nuclear DNA (blue). Scale bar; 10 µm.

nuclei (Fig. 3d–o).

Next, we reconstructed 3D-images of the nuclei from a series of 2D-image stacks with successive sections recorded for each cell (Fig. 4), and evaluated the relative positioning of *Zscan4* and RP23-240D19 in CT7 (Table 1). Notably, *Zscan4* loci in the early embryos at the 1-, 2-, and 4-cell stages were located peripherally in CT7s, at significantly higher frequencies of 78.6%, 93.5%, and 84.0%, respectively, while they were preferentially located in the interior of CT7s in fibroblasts. Similar to the early embryos, in ES cells, 76.9% of *Zscan4* loci were located peripherally in CT7s. Interestingly, another G-positive banded region on chromosome 7, detected by probe RP23-240D19, showed the reverse positioning to *Zscan4*. RP23-240D19 in the early embryos and ES cells were located inside CT7s at a significantly lower frequency, while in fibroblasts, RP23-240D19 was preferentially located peripherally. Furthermore, for the quantitative evaluation of relative CT structures, we measured the volume of the CT7s in the early embryos, ES cells, and fibroblasts (Table 1). The mean values for the volume of CT7 at the 1-, 2-, and 4-cell stages were 368.8 µm^3, 288.3 µm^3 and 208.2 µm^3 on average, respectively. In contrast, ES cells and fibroblasts showed significantly different values of 11.2 µm^3 and 17.3 µm^3 on average, respectively. Therefore, the CT7 of the embryos was much larger than those of ES cells and fibroblasts.

Table 1. Localization of *Zscan4* and RP23-240D19, and volume of chromosome territory (CT) 7 in the early embryos, embryonic stem (ES) cells and fibroblasts

Stage/type of cells	Frequency of localization on CT7 surface		Average volume of CT7 ± S.D. (µm^3)
	Zscan4	RP23-240D19	
1-cell	78.6% (11/14) [a]	35.3% (6/17) [c]	368.8 ± 303.9 [e]
2-cell	93.5% (29/31) [a]	38.1% (8/21) [c]	288.3 ± 287.6 [e]
4-cell	84.0% (21/25) [a]	40.0% (14/35) [c]	208.2 ± 175.8 [e]
ES cell	76.9% (30/39) [a]	20.8% (5/24) [c]	11.2 ± 6.4 [f]
Fibroblast	31.0% (13/42)[b]	79.5% (35/44) [d]	17.3 ± 11.4 [f]

Values with different superscripts within each column are significantly different at $P < 0.01$.

Discussion

Chamber device for 3D-FISH in early embryos (EASI-FISH chamber)

In this study, we devised a FISH chamber suitable for 3D-FISH in the early embryos. To date, 3D-FISH analysis in oocytes and embryos has been confined to a few reports [3, 4, 10–12, 24]. The reasons for the limitations of the studies were the unique morphological and cytological properties of the embryos. Hence, for FISH analysis, the embryos are put on the glass with a little amount of solution and firmly adhered by air-drying [25–28]. However, in such protocols, the 3D structure of the interphase nucleus is liable to be disrupted by the physical pressure of mounting, such that it becomes difficult to evaluate the detailed spatial arrangements. Yet, dewatering the embryo could enhance undesirable non-specific signals. Alternatively, a method of processing the embryos in a floating state using metal rings has been applied; however, this operation is complicated and might influence the detection of the signals because of inadequate buffer treatments [10, 24].

Then, we aimed to develop a convenient 3D-FISH technique for early mouse embryos. To acquire the distinct signals from the nuclei of the early embryos in 3D-FISH, the following are required: (i) a spacer to maintain the higher-order structure of the nuclei throughout the process of mounting and hybridization; (ii) adhesion of the embryos onto the coverslips; and (iii) treatment of the embryos with a sufficient volume of buffer solutions. To adapt the current 3D-FISH process in somatic cells to early embryos, we developed a chamber device (Fig. 1). The PLL-coated surface of the coverslip allows the embryos to adhere onto the chamber glass firmly and the frame of the chamber maintains the 3D structure of the interphase nucleus, which permits the measurement of various kinds of spatial arrangements in the nucleus precisely. This chamber would allow researchers with limited experience in handling embryos to carry out 3D-FISH similarly to cultured cells, so that the optimal 3D-FISH protocol for specimens can be designed by adjusting the conditions of pepsin permeation, elution, and other steps. For example, increasing the concentration of the chromosome painting probes to 1.75-fold and an extended period of hybridization for 5 days to permeate probes to the specimens resulted in enhanced signal detection.

Visualization of spatial arrangements in the interphase nucleus

The spatial arrangement of CTs is closely related to nuclear function and gene expression [5]. The size and genetic density of the chromosome are involved in an allocation of CTs, termed "radial arrangement (radial positioning)" [6, 7]. Larger chromosomes are located preferentially under the nuclear membrane and smaller ones are located in the interior in the nucleus [6]. The genetic density of a chromosome also influences its allocation. In humans, even though the sizes of chromosome 18 and 19 are almost equivalent, chromosome 18, with a low genetic density, lies on the periphery, whereas, chromosome 19, with a high genetic density, is located in the interior of the nucleus [7, 21]. It has been reported that in human T lymphocytes, CTs will relocate in association with cell differentiation [8], which is the so-called "relative arrangement". Structurally, the peripheral zone of a CT is mostly formed by euchromatin and in general, the nuclear matrix and peripheral zone of CTs are in a transcriptionally active state [5]. Moreover, higher-order sub-chromosomal domains, termed "topologically associating domains (TADs)", interact with each other [29–31]. Therefore, this implied that "radial arrangement" and "relative arrangement", as well as "TADs" in CTs are involved intrinsically in the dynamic process of the early development.

With regard to the higher-order nuclear organization in early embryos, spatial arrangements of the pericentromeric regions and telomeres in the interphase nuclei of mice have been reported [3, 4, 12]. These studies revealed that, in contrast to somatic cells, after fertilization until the mid-2-cell stage the embryos have a very peculiar nuclear organization, with highly decondensed pericentromeric regions located over the nucleolar precursor bodies (NPBs), and enter a transcriptionally active state; NPBs are essential for early mammalian development [32]. Koehler *et al*. [10] demonstrated the relocation of CTs during the 8- to 16-cell stages in bovine preimplantation embryos when ZGA occurs. Gene-rich chromosome 19 and gene-poor chromosome 20 have an equivalent size and show the same radial arrangement until the 8-cell stage; however, thereafter, CT19 is relocated more internally and CT20 is located peripherally in the nucleus.

Here, we visualized the pericentromeric/centromeric regions, certain gene loci, and CTs in the mouse early embryos simultaneously for the first time using 3D-FISH, and obtained comprehensive information concerning their spatial arrangements. We focused on *Zscan4*, which is located next to the pericentromeric heterochromatin of chromosome 7 and is transiently expressed at the late-2-cell stage upon ZGA. Our results demonstrated that pericentromeric/centromeric regions became reorganized and associated with NLBs during the early cleavage stage (Fig. 3a–c), as was reported previously [3]. Upon ZGA, major satellite repeats in the pericentromeric regions are highly expressed at the 2-cell stage and promptly become silent until the 4-cell stage [4], indicating that the chromosomal structure in the pericentromeric domains at the 2-cell stage is transcriptionally active. Furthermore, chromosome 7 became very enlarged compared with that of somatic cells and gathered around NLBs with a deformed shape (Figs. 3 and 4 and Table 1). In somatic cells, transcription occurs in the spotted "transcription factories" in a nucleus, as detected by accumulation of RNA polymerases [33]. By contrast, in early embryos, global gene expression occurs together upon ZGA and RNA polymerases distribute broadly in the nucleus without distinct transcription factories [34]. Thus, conformational transition, such as the remarkable enlargement of CTs, and loosening and clustering of pericentromeric heterochromatin around NLBs in the early embryos, seems to create a genomic environment that is ready to induce genome-wide gene expression upon ZGA. Besides the reorganization of chromatin, such as pericentromeric domains and CTs, the relative positioning of *Zscan4* loci in CT7s during the early cleavages was investigated (Fig. 4 and Table 1). Interestingly, *Zscan4* loci in the early embryos were mostly located peripherally in CT7s, which contrasted with *Zscan4*'s interior localization in fibroblasts. Taken together, transient expression of *Zscan4* at the 2-cell stage might be regulated by the cooperative chromosomal modifications. Accompanied by the enlargement of CT7 and peripheral localization of *Zscan4*, pericentromeric regions began remodeling into a condensed form of chromatin at the late 2-cell [12] and changed to heterochromatin at the 4-cell stage (Fig. 3a–c), by which *Zscan4* may be transcriptionally silenced. Our experiments also demonstrated a peripheral localization of *Zscan4* in CT7 in ES cells (Fig. 4d). As the pericentromeric domains of *Zscan4*-expressing ES cells became loosened and distributed along the nucleoli [35], the peripheral localization of *Zscan4* in CT7 might be a precondition for activating *Zscan4* in ES cells. We additionally examined the distribution of another G-positive banded region detected by probe RP23-240D19 on 7qE1. Interestingly, RP23-240D19 showed the reverse positioning to *Zscan4* (Table 1). However, the reason for the relocation of RP23-240D19 to the surface of CT7 in fibroblasts remains to be determined.

In this study, we investigated the dynamics of higher-order nuclear architecture of embryos during the MZT period by the 3D-FISH technique using a new "EASI-FISH" chamber. Our results indicated that the structural alteration and spatial arrangement in the nucleus participate cooperatively in regulating genomic function during ZGA. Consequently, 3D-FISH for embryos provides visualized information that is difficult to acquire from chromosome conformation capture (3C) and chromosome conformation capture (3C)-based

high-throughput method (Hi-C) analyses. This convenient and reproducible 3D-FISH technique can be applied to other valuable tools, such as 3D-RNA-FISH and 3D-immuno-FISH, to investigate further the nuclear dynamics governing genomic function in highly organized developmental phenomena.

Acknowledgements

This work was supported by JSPS KAKENHI (Grant Numbers JP23658228 to TM and JP24613003 to HT). The authors thank Kayoko Suenaga of Carl Zeiss Microscopy Co., Ltd. for technical assistance and Naomi Kamimura-Backes for proof-reading this manuscript. Idiomatic illustration of mouse chromosome 7 was cited from Idiogram Album (http://www.pathology.washington.edu/research/cytopages/idiograms/mouse/) provided by Dr. David Adler, University of Washington. None of the authors has any conflict of interest to declare.

References

1. **Cremer T, Zakhartchenko V.** Nuclear architecture in developmental biology and cell specialisation. *Reprod Fertil Dev* 2011; **23**: 94–106. [Medline] [CrossRef]
2. **Borsos M, Torres-Padilla ME.** Building up the nucleus: nuclear organization in the establishment of totipotency and pluripotency during mammalian development. *Genes Dev* 2016; **30**: 611–621. [Medline] [CrossRef]
3. **Aguirre-Lavin T, Adenot P, Bonnet-Garnier A, Lehmann G, Fleurot R, Boulesteix C, Debey P, Beaujean N.** 3D-FISH analysis of embryonic nuclei in mouse highlights several abrupt changes of nuclear organization during preimplantation development. *BMC Dev Biol* 2012; **12**: 30. [Medline] [CrossRef]
4. **Probst AV, Okamoto I, Casanova M, El Marjou F, Le Baccon P, Almouzni G.** A strand-specific burst in transcription of pericentric satellites is required for chromocenter formation and early mouse development. *Dev Cell* 2010; **19**: 625–638. [Medline] [CrossRef]
5. **Cremer T, Cremer M.** Chromosome territories. *Cold Spring Harb Perspect Biol* 2010; **2**: a003889. [Medline] [CrossRef]
6. **Sun HB, Shen J, Yokota H.** Size-dependent positioning of human chromosomes in interphase nuclei. *Biophys J* 2000; **79**: 184–190. [Medline] [CrossRef]
7. **Tanabe H, Müller S, Neusser M, von Hase J, Calcagno E, Cremer M, Solovei I, Cremer C, Cremer T.** Evolutionary conservation of chromosome territory arrangements in cell nuclei from higher primates. *Proc Natl Acad Sci USA* 2002; **99**: 4424–4429. [Medline] [CrossRef]
8. **Kim SH, McQueen PG, Lichtman MK, Shevach EM, Parada LA, Misteli T.** Spatial genome organization during T-cell differentiation. *Cytogenet Genome Res* 2004; **105**: 292–301. [Medline] [CrossRef]
9. **Amano T, Sagai T, Tanabe H, Mizushina Y, Nakazawa H, Shiroishi T.** Chromosomal dynamics at the *Shh* locus: limb bud-specific differential regulation of competence and active transcription. *Dev Cell* 2009; **16**: 47–57. [Medline] [CrossRef]
10. **Koehler D, Zakhartchenko V, Froenicke L, Stone G, Stanyon R, Wolf E, Cremer T, Brero A.** Changes of higher order chromatin arrangements during major genome activation in bovine preimplantation embryos. *Exp Cell Res* 2009; **315**: 2053–2063. [Medline] [CrossRef]
11. **Bonnet-Garnier A, Feuerstein P, Chebrout M, Fleurot R, Jan HU, Debey P, Beaujean N.** Genome organization and epigenetic marks in mouse germinal vesicle oocytes. *Int J Dev Biol* 2012; **56**: 877–887. [Medline] [CrossRef]
12. **Probst AV, Santos F, Reik W, Almouzni G, Dean W.** Structural differences in centromeric heterochromatin are spatially reconciled on fertilisation in the mouse zygote. *Chromosoma* 2007; **116**: 403–415. [Medline] [CrossRef]
13. **Zeng F, Schultz RM.** RNA transcript profiling during zygotic gene activation in the preimplantation mouse embryo. *Dev Biol* 2005; **283**: 40–57. [Medline] [CrossRef]
14. **Falco G, Lee SL, Stanghellini I, Bassey UC, Hamatani T, Ko MS.** *Zscan4*: a novel gene expressed exclusively in late 2-cell embryos and embryonic stem cells. *Dev Biol* 2007; **307**: 539–550. [Medline] [CrossRef]
15. **Matsson H, Davey EJ, Draptchinskaia N, Hamaguchi I, Ooka A, Levéen P, Forsberg E, Karlsson S, Dahl N.** Targeted disruption of the ribosomal protein S19 gene is lethal prior to implantation. *Mol Cell Biol* 2004; **24**: 4032–4037. [Medline] [CrossRef]
16. **Ma M, Zhou L, Guo X, Lv Z, Yu Y, Ding C, Zhang P, Bi Y, Xie J, Wang L, Lin M, Zhou Z, Huo R, Sha J, Zhou Q.** Decreased cofilin 1 expression is important for compaction during early mouse embryo development. *Biochim Biophys Acta* 2009; **1793**: 1804–1810. [CrossRef]
17. **Anzai M, Nishiwaki M, Yanagi M, Nakashima T, Kaneko T, Taguchi Y, Tokoro M, Shin SW, Mitani T, Kato H, Matsumoto K, Nakagata N, Iritani A.** Application of laser-assisted zona drilling to in vitro fertilization of cryopreserved mouse oocytes with spermatozoa from a subfertile transgenic mouse. *J Reprod Dev* 2006; **52**: 601–606. [Medline] [CrossRef]
18. **Mizuno S, Sono Y, Matsuoka T, Matsumoto K, Saeki K, Hosoi Y, Fukuda A, Morimoto Y, Iritani A.** Expression and subcellular localization of GSE protein in germ cells and preimplantation embryos. *J Reprod Dev* 2006; **52**: 429–438. [Medline] [CrossRef]
19. **Weier HU, Zitzelsberger HF, Gray JW.** Non-isotopical labeling of murine heterochromatin in situ by hybridization with in vitro-synthesized biotinylated gamma (major) satellite DNA. *Biotechniques* 1991; **10**: 498–502: 504–505. [Medline]
20. **Telenius H, Pelmear AH, Tunnacliffe A, Carter NP, Behmel A, Ferguson-Smith MA, Nordenskjöld M, Pfragner R, Ponder BA.** Cytogenetic analysis by chromosome painting using DOP-PCR amplified flow-sorted chromosomes. *Genes Chromosomes Cancer* 1992; **4**: 257–263. [Medline] [CrossRef]
21. **Cremer M, von Hase J, Volm T, Brero A, Kreth G, Walter J, Fischer C, Solovei I, Cremer C, Cremer T.** Non-random radial higher-order chromatin arrangements in nuclei of diploid human cells. *Chromosome Res* 2001; **9**: 541–567. [Medline] [CrossRef]
22. **Solovei I, Walter J, Cremer M, Schermelleh L.** FISH on three-dimensionally preserved nuclei. *In*: Squire J, Beatty B, Mai S (eds.), FISH: a Practical Approach. Oxford University Press, Oxford; 2002: 119–157.
23. **Kawamura R, Tanabe H, Wada T, Saitoh S, Fukushima Y, Wakui K.** Visualization of the spatial positioning of the SNRPN, UBE3A, and GABRB3 genes in the normal human nucleus by three-color 3D fluorescence in situ hybridization. *Chromosome Res* 2012; **20**: 659–672. [Medline] [CrossRef]
24. **Popken J, Koehler D, Brero A, Wuensch A, Guengoer T, Thormeyer T, Wolf E, Cremer T, Zakhartchenko V.** Positional changes of a pluripotency marker gene during structural reorganization of fibroblast nuclei in cloned early bovine embryos. *Nucleus* 2014; **5**: 542–554. [Medline] [CrossRef]
25. **Bielanska M, Tan SL, Ao A.** Fluorescence in-situ hybridization of sex chromosomes in spermatozoa and spare preimplantation embryos of a Klinefelter 46,XY/47,XXY male. *Hum Reprod* 2000; **15**: 440–444. [Medline] [CrossRef]
26. **Alberio R, Brero A, Motlík J, Cremer T, Wolf E, Zakhartchenko V.** Remodeling of donor nuclei, DNA-synthesis, and ploidy of bovine cumulus cell nuclear transfer embryos: effect of activation protocol. *Mol Reprod Dev* 2001; **59**: 371–379. [Medline] [CrossRef]
27. **Okamoto I, Otte AP, Allis CD, Reinberg D, Heard E.** Epigenetic dynamics of imprinted X inactivation during early mouse development. *Science* 2004; **303**: 644–649. [Medline] [CrossRef]
28. **Namekawa SH, Lee JT.** Detection of nascent RNA, single-copy DNA and protein localization by immunoFISH in mouse germ cells and preimplantation embryos. *Nat Protoc* 2011; **6**: 270–284. [Medline] [CrossRef]
29. **Linhoff MW, Garg SK, Mandel G.** A high-resolution imaging approach to investigate chromatin architecture in complex tissues. *Cell* 2015; **163**: 246–255. [Medline] [CrossRef]
30. **Fraser J, Ferrai C, Chiariello AM, Schueler M, Rito T, Laudanno G, Barbieri M, Moore BL, Kraemer DC, Aitken S, Xie SQ, Morris KJ, Itoh M, Kawaji H, Jaeger I, Hayashizaki Y, Carninci P, Forrest AR, Semple CA, Dostie J, Pombo A, Nicodemi M. FANTOM Consortium**. Hierarchical folding and reorganization of chromosomes are linked to transcriptional changes in cellular differentiation. *Mol Syst Biol* 2015; **11**: 852. [Medline] [CrossRef]
31. **Franke M, Ibrahim DM, Andrey G, Schwarzer W, Heinrich V, Schöpflin R, Kraft K, Kempfer R, Jerković I, Chan WL, Spielmann M, Timmermann B, Wittler L, Kurth I, Cambiaso P, Zuffardi O, Houge G, Lambie L, Brancati F, Pombo A, Vingron M, Spitz F, Mundlos S.** Formation of new chromatin domains determines pathogenicity of genomic duplications. *Nature* 2016; **538**: 265–269. [Medline] [CrossRef]
32. **Ogushi S, Palmieri C, Fulka H, Saitou M, Miyano T, Fulka J Jr.** The maternal nucleolus is essential for early embryonic development in mammals. *Science* 2008; **319**: 613–616. [Medline] [CrossRef]
33. **Rieder D, Trajanoski Z, McNally JG.** Transcription factories. *Front Genet* 2012; **3**: 221. [Medline] [CrossRef]
34. **Tokoro M, Shin SW, Nishikawa S, Lee HH, Hatanaka Y, Amano T, Mitani T, Kato H, Anzai M, Kishigami S, Saeki K, Hosoi Y, Iritani A, Matsumoto K.** Deposition of acetylated histones by RNAP II promoter clearance may occur at onset of zygotic gene activation in preimplantation mouse embryos. *J Reprod Dev* 2010; **56**: 607–615. [Medline] [CrossRef]
35. **Akiyama T, Xin L, Oda M, Sharov AA, Amano M, Piao Y, Cadet JS, Dudekula DB, Qian Y, Wang W, Ko SB, Ko MS.** Transient bursts of Zscan4 expression are accompanied by the rapid derepression of heterochromatin in mouse embryonic stem cells. *DNA Res* 2015; **22**: 307–318. [Medline] [CrossRef]